

Type Synthesis and Dynamics Performance Evaluation of a Class of 5-DOF Redundantly Actuated Parallel Mechanisms

Bing-Shan Jiang Hai-Rong Fang Hai-Qiang Zhang

School of Mechanical, Electronic and Control Engineering, Beijing Jiaotong University, Beijing 100044, China

Abstract: This paper presents a five degree of freedom (5-DOF) redundantly actuated parallel mechanism (PM) for the parallel machining head of a machine tool. A 5-DOF single kinematic chain is evolved into a secondary kinematic chain based on Lie group theory and a configuration evolution method. The evolutionary chain and four 6-DOF kinematic chain SPS (S represents spherical joint and P represents prismatic joint) or UPS (U represents universal joint) can be combined into four classes of 5-DOF redundantly actuated parallel mechanisms. That SPS-(2UPR)R (R represents revolute joint) redundantly actuated parallel mechanism is selected and is applied to the parallel machining head of the machine tool. All formulas of the 4SPS-(2UPR)R mechanism are deduced. The dynamic model of the mechanism is shown to be correct by Matlab and automatic dynamic analysis of mechanical systems (ADAMS) under no-load conditions. The dynamic performance evaluation indexes including energy transmission efficiency and acceleration performance evaluation are analyzed. The results show that the 4SPS-(2UPR)R mechanism can be applied to a parallel machining head and have good dynamic performance.

Keywords: Type synthesis, redundantly actuated parallel mechanism (PM), lie group theory, configuration evolution, dynamics performance evaluation.

1 Introduction

Parallel mechanisms (PMs) have begun to be manufactured into parallel machining heads and be applied to the high-precision machine tool, such as Sprint Z3^[1], Tricept^[2], Exechon^[3]. The Sprint Z3, Tricept and Exechon are 3-degree of freedom (DOF) parallel machining heads. There are few five degrees of freedom (5-DOF) redundantly actuated parallel machining heads. The 5-DOF parallel machining head will be expected to complete the process task at a high velocity^[4,5], high-precision^[6], high-security and high-performance^[7] when the machine tool is processing workpieces. It is important to ensure high-security and high-performance of the 5-DOF parallel machining head, otherwise, it will be more destructive to work pieces. Some researchers try to add redundant actuation^[8-11] to the parallel mechanism (PM) to improve fault tolerance, security, high-performance and stability. Contrasted with the traditional parallel mechanisms, the redundantly actuated parallel mechanisms can reduce singularity, increase effective workspace and improve security. It has high-security, high-performance, high fault tolerance and fewer singularities. Therefore, it is a worth-

while task to design the 5-DOF redundantly actuated parallel mechanism with good dynamic performance.

Some researchers have researched the 5-DOF parallel mechanism. Qu^[12] selected the single-loop mechanism or the multi-loop mechanism as an actuated unit and completed the constraint couple of the kinematic chain to obtain the non-over-constrained or low-over-constrained redundantly actuated parallel mechanism. Chen et al.^[13] proposed a 4UPS (U represents universal joint, P represents prismatic joint, S represents spherical joint)-RPU (R represents revolute joint) 5-DOF parallel mechanism, and studied the influence of different performance indexes on a task workspace and optimized the parallel mechanism's parameters. Chen et al.^[14] designed a 4UPS-UPU 5-DOF parallel mechanism and established a dynamic mathematical model of the mechanism by the principle of virtual work. Lu et al.^[15,16] designed two 5-DOF parallel mechanisms and deduced formulas of displacement, velocity and acceleration of the mechanism. The dynamic model with friction considered is established by the principle of virtual tests and the mathematical model is verified to be correct. Yao et al.^[17] established a dynamic mathematical model of the 5UPS-PRPU redundantly actuated parallel mechanism through the Lagrange method and optimized the actuated moment. The dynamic mathematical model was verified to be correct by theory analysis and simulated experiments. Liu et al.^[18] designed a 6PUS-UPU redundantly actuated parallel mechanism and established

Research Article

Manuscript received May 19, 2020; accepted September 16, 2020; published online December 23, 2020

Recommended by Associate Editor Xun Xu

© Institute of Automation, Chinese Academy of Sciences and Springer-Verlag GmbH Germany, part of Springer Nature 2020

the generalized pseudo-inverse Jacobi matrix of global dynamic models by the principle of virtual work. The control model of the parallel mechanism is analyzed by the force-position hybrid control strategy. Song et al.^[19] designed a T5 parallel mechanism and established the elastic dynamics model of the T5 parallel mechanism. Jiang et al.^[20] designed a class of 5-DOF parallel mechanisms with large output rotational angles and analyzed kinematics performance of parallel mechanisms. Guo et al.^[21] designed 4-CPS-RPS (C represents cylindrical joint) parallel mechanism and researched the proportional-integral-derivative (PID) control and the force-position redundant control. Masouleh et al.^[22,23] analyzed the kinematics of the 5-RPUR parallel mechanisms. Saadatzi et al.^[24] used a geometric interpretation of the so-called vertex space and analyzed the workspace of the 5-PRUR parallel mechanisms. Xie et al.^[25] designed a 5-DOF parallel mechanism and optimized parameters of the mechanism. Wang et al.^[26] designed a 5UPS-RPS parallel mechanism and analyzed the velocity global performance index of this parallel mechanism. Jin et al.^[27] proposed a novel method about the synthesis of generalized parallel mechanisms (GPMs) and designed a class of novel 5-DOF generalized parallel mechanisms with high performance.

In the above research, there are mostly 5-DOF traditional parallel mechanisms and few 5-DOF redundantly actuated parallel mechanisms. Most researchers directly design 5-DOF traditional parallel mechanisms, but few researchers research dynamics performance evaluation of a class of 5-DOF redundantly actuated parallel mechanisms. But most traditional parallel mechanisms have low fault tolerance and many singularities. In order to design a feasible parallel machining head, this paper will research type synthesis of the redundantly actuated parallel mechanism and analyze dynamic performance of the 5-DOF redundantly actuated parallel mechanism as the machining head.

In this paper, one 5-DOF single kinematic chain is evolved into one first-order kinematic chain including two secondary kinematic chains by Lie group theory method

and configuration evolution method. The evolutionary kinematic chain and four 6-DOF kinematic chain SPS or UPS are selected and combined into four classes of redundantly actuated parallel mechanisms in Section 2. The 4SPS-(2UPR)R redundantly actuated parallel mechanism comes from one of four classes of mechanisms and is applied to the parallel machining head. The position, velocity and acceleration of the 4SPS-(2UPR)R mechanism are deduced in Section 3. Dynamic mathematical equations of the 4SPS-(2UPR)R mechanisms are established by the principle of virtual work. A simplified dynamic mathematical model of the 4SPS-(2UPR)R mechanism is obtained and is shown to be correct by Matlab and automatic dynamic analysis of mechanical systems (ADAMS) under no-load conditions in Section 4. The fifth part introduces a dynamic acceleration evaluation index and energy transmission efficiency index. Combined with application numerical examples and parameters of the 4SPS-(2UPR)R mechanism, acceleration performance and transfer efficiency of the mechanism is analyzed. Finally, the article is summarized in Section 6.

2 Type synthesis of the mechanism

2.1 Lie group theory

Lie group theory can describe collections of all rigid body motions. Jin^[28] gives twelve classes of displacement subgroups including $G(x)$ in space. $G(x)$ represents that two-dimensional movement is perpendicular to the line x and one-dimensional rotation is rotated to the line x . $G(x)$ is shown in Table 1. 5-DOF kinematic chains can be obtained by adding translational joints and revolute joints when $G(x)$ is considered as one group. 5-DOF kinematic chains are shown in Table 2. $T(x)$ (T represents translational joint), $G(x)$ and $R(N, y)$ can be exchanged as one group, but they are not internally exchanged. x , y and z are axis directions of motion joints. N_1 , N_2 and N_3 are position of motion joints.

Table 1 $G(x)$ kinematic chains

Displacement subgroups	Kinematic chains	Displacement subgroups	Kinematic chains
$R(N_1, x)R(N_2, x)R(N_3, x)$	$^xR^xR^xR$	$R(N_1, x)T(x)T(y)$	$^xR^xP^yP$
$T(y)R(N_1, x)R(N_2, x)$	$^yP^xR^xR$	$T(x)R(N_1, x)T(y)$	$^xP^xR^yP$
$R(N_1, x)T(y)R(N_2, x)$	$^xR^yP^xR$	$T(x)T(y)R(N_1, x)$	$^xP^yP^xR$
$R(N_1, x)R(N_2, x)T(y)$	$^xR^xR^yP$		

Table 2 5-DOF kinematic chains

5-DOF displacement subgroups	Kinematic chains
$\{T(x)\}G(x)\{R(N_1, y)\}$	$^xP[^yP^xP^xR]^yR^xP[^yP^xR^xR]^yR^xP[^xR^xR^xR]^yR$
$G(x)\{T(x)\}\{R(N_1, y)\}$	$[^xR^xR^xR]^xP^yR[^yP^xR^xR]^xP^yR[^yP^xP^xR]^xP^yR$
$\{R(N_1, y)\}\{R(N_2, y)\}G(x)$	$^yR^yR[^xR^xR^xR]^yR^yR[^yP^xR^xR]^yR^yR[^yP^xP^xR]^yR$
$\{R(N_1, y)\}G(x)\{R(N_2, y)\}$	$^yR[^xR^xR^xR]^yR^yR[^yP^xR^xR]^yR^yR[^yP^xP^xR]^yR$

2.2 Configuration evolution

Configuration evolution is an effective method for designing the redundantly actuated parallel mechanism and obtaining new redundantly actuated parallel mechanisms to satisfy specific requirements. Fan et al. [29] have evolved a planar 6R mechanism into 4-DOF parallel mechanisms.

In order to configure type synthesis of the redundantly actuated parallel mechanism, each 5-DOF kinematic chain is shown in Table 2. $G(x)$ is replaced with the $^xR^xR^xR$, 5-DOF kinematic chain in Table 2 can be expressed as Fig. 1. Without changing the freedom of the 5-DOF kinematic chain, $T(x)$, $G(x)$, $R(N, y)$ can be exchanged as one group, but they are not internally exchanged. Two $G(x)$ are connected in parallel, the 3R open-loop chain is developed into a 6R closed-loop chain, each kinematic chain in Fig. 1 is evolved into a kinematic chain in Fig. 2. One kinematic chain is developed into one first-order kinematic chain including two secondary kinematic chains. In order to maintain large rotational angles and workspaces, the evolutionary kinematic chain in Table 2 is shown in Table 3.

In general, each kinematic chain of the parallel mechanism has only one actuated joint, it is mounted on the base or the adjacent joint. The 5-DOF redundantly actuated parallel mechanism should have six kinematic chains

to place six actuated joints. Each kinematic chain in Table 3 is selected as one first-order kinematic chain, and each kinematic chain includes two secondary kinematic chains, then four kinematic chains SPS or UPS are selected as the third, fourth, fifth and sixth kinematic chains. The above six kinematic chains connect the moving platform with the fixed platform, respectively. Four kinematic chains SPS or UPS are symmetrically arranged in the center, and evolutionary kinematic chains are axially symmetric. Because the 6-DOF kinematic chain is an unconstrained kinematic chain, the evolutionary kinematic chain determines DOF of the redundantly actuated parallel mechanism. Each kinematic chain in Table 3 can be selected, each kinematic chain and four unconstrained kinematic chains can be combined into a 5-DOF redundantly actuated parallel mechanism. The new 5-DOF redundantly actuated parallel mechanism is shown in Table 4.

3 Kinematics analysis

3.1 Description of redundantly actuated parallel mechanism

The redundantly actuated parallel mechanism is selec-

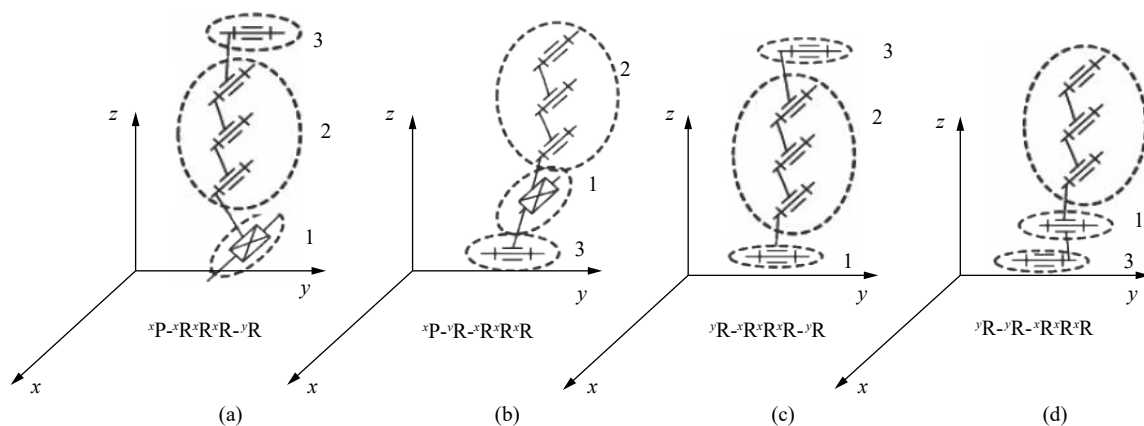


Fig. 1 Four classes of 5-DOF kinematic chains

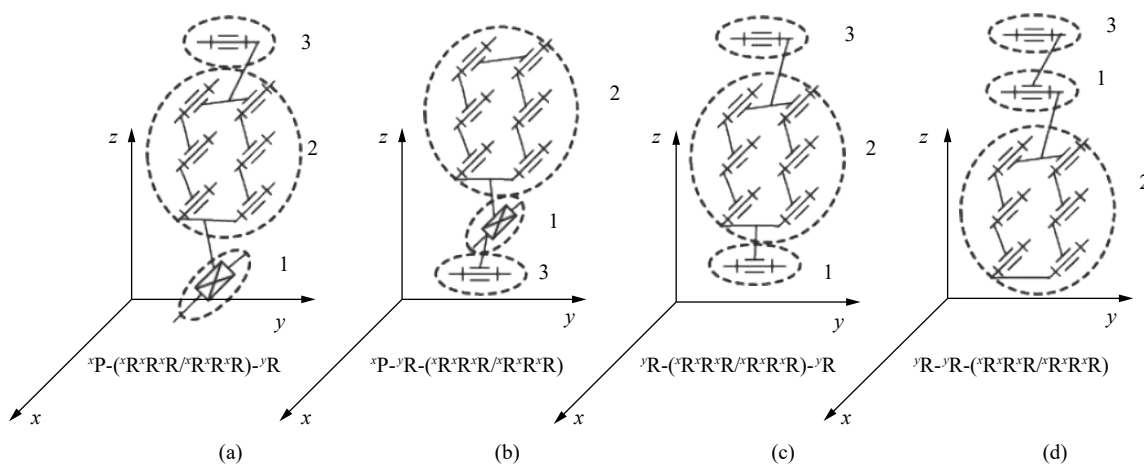


Fig. 2 5-DOF kinematic chains

Table 3 5-DOF kinematic chains

Kinematic chains	Evolutionary kinematic chains	Kinematic chains	Evolutionary kinematic chains
(a) ${}^xP-\{ {}^xR^xR^xR/^xR^xR^xR \} - {}^yR$	$\{ {}^xPyP^xR^xR/^xPyP^xR^xR \} - {}^yR$	(b) $\{ {}^xR^xR^xR/^xR^xR^xR \} - {}^xP- {}^yR$	$\{ {}^yPz^xPC/^xRz^xPC \} - {}^yR$
	$\{ {}^xPz^xR^xR/^xPz^xR^xR \} - {}^yR$		$\{ {}^xR^xR^xC/^xR^xR^xC \} - {}^yR$
	$\{ {}^xPyP^zP^xR/^xPyP^zP^xR \} - {}^yR$		$\{ {}^xR^yP^xC/^xR^yP^xC \} - {}^yR$
	$\{ {}^xC^xR^xR/^xC^xR^xR \} - {}^yR$		$\{ {}^yPz^xPC/^yPz^xPC \} - {}^yR$
	$\{ {}^xC^yP^xR/^xC^yP^xR \} - {}^yR$		$\{ {}^xR^yP^xR^xP/^xR^yP^xR^xP \} - {}^yR$
	$\{ {}^xC^zP^xR/^xC^zP^xR \} - {}^yR$		$\{ {}^xR^zP^xR^xP/^xR^zP^xR^xP \} - {}^yR$
	$\{ {}^xC^zP^yP/^xC^zP^yP \} - {}^yR$		$\{ {}^xR^yP^zP^xP/^xR^yP^zP^xP \} - {}^yR$
(c) ${}^yR-\{ {}^xR^xR^xR/^xR^xR^xR \} - {}^yR$	$\{ {}^yU^xR^xR/^yU^xR^xR \} - {}^yR$	(d) $\{ {}^xR^xR^xR/^xR^xR^xR \} - {}^yR- {}^yR$	$\{ {}^yP^xR^xR/^yP^xR^xR \} - {}^yR$
	$\{ {}^yU^xP^xR/^yU^xP^xR \} - {}^yR$		$\{ {}^zP^xR^xR/^zP^xR^xR \} - {}^yR$
	$\{ {}^yU^xyP^xR/^yU^xyP^xR \} - {}^yR$		$\{ {}^yP^zP^xR/^yP^zP^xR \} - {}^yR$
	$\{ {}^yU^xP^yP/^yU^xP^yP \} - {}^yR$		$\{ {}^yP^xR^xU/^yP^xR^xU \} - {}^yR$
	$\{ {}^yU^xyP^xR/^yU^xyP^xR \} - {}^yR$		$\{ {}^zP^xR^xU/^zP^xR^xU \} - {}^yR$
	$\{ {}^yC^xR^xR/^yC^xR^xR \} - {}^yR$		$\{ {}^zP^yP^xU/^zP^yP^xU \} - {}^yR$
	$\{ {}^yC^xP^xR/^yC^xP^xR \} - {}^yR$		$\{ {}^xR^xR^xU/^xR^xR^xU \} - {}^yR$
			$\{ {}^zP^xR^yC/^zP^xR^yC \} - {}^yR$
			$\{ {}^xR^xR^yC/^xR^xR^yC \} - {}^yR$
			$\{ {}^zP^xR^yC/^zP^xR^yC \} - {}^yR$

ted as the parallel machining head according to the following criteria: 1) The actuated joint is mounted on the base or near the base. 2) In order to maintain fast response movement of the moving platform, the prismatic joint should be selected as the actuated joint. 3) The translation workspace in the vertical direction may be limited by the range of linear actuators. The 4SPS-(2UPR)R parallel mechanism is more suitable for the machining head. The model of 4SPS-(2UPR)R is shown in Fig. 3. The 4SPS-(2UPR)R is composed of five first-order kinematic chains, the fixed platform and the moving platform. Five first-order kinematic chains include four first-order kinematic chains SPS and (2UPR)R kinematic chains. The (2UPR)R includes two secondary kinematic chains SPR and a single rotated joint R, the single rotated joint R is named as H. The axis of the single rotation joint R is perpendicular to the axis of the rotated joint R of the SPR. The first-order kinematic chain SPS is an unconstrained kinematic chain. The first-order kinematic chain (2UPR)R is a 5-DOF kinematic chain. 4SPS-(2UPR)R is a 3t2r (t denotes translation and r denotes rotation) redundantly actuated parallel mechanism when H is parallel to the fixed platform. 4SPS-(2UPR)R is a 2t3r^[30] redundantly actuated parallel mechanism when H is not parallel to the fixed platform.

All A_i coordinates are set on the fixed platform, all B_i coordinates are set on the moving platform in Fig. 4, $i=1, \dots, 6$. The fixed coordinate system O -XYZ is in the center of the fixed platform. A_1 and A_2 are on the OX -axis, A_1 and A_2 are symmetric along OY -axis. The mov-

ing coordinate system o -uvw is in the center of the moving platform. The o point is in the center of the moving platform. B_1 and B_2 are on the ou -axis, B_1 and B_2 are symmetric along ov -axis. The O point of O -XYZ to A_i is $\frac{D}{2}$, $i=1, 2$. The O point of O -XYZ to the point A_i is D , $i=3, \dots, 6$. The o point of o -uvw to B_i is $\frac{d}{2}$, $i=1, 2$. The o point of o -uvw to the point B_i is d , $i=3, \dots, 6$. The initial length of each kinematic chain is l_{i0} , $i=1, \dots, 6$. The P joint of each kinematic chain is selected as the actuated joint.

3.2 Position analysis

The O coordinate is $(0, 0, 0)^T$ in O -XYZ, it is expressed as ${}^OO=(0, 0, 0)^T$. The o coordinate is $(x, y, z)^T$ in O -XYZ, it is expressed as ${}^Oo=(a, b, c)^T$. $A_1B_1B_2A_1$ is considered as the plane closed-loop mechanism. Four R joints of the plane closed-loop mechanism correspond to three Euler angles, there are α, β, γ . $R_\alpha, R_{\beta_1}, R_{\beta_2}, R_\gamma$ is the vector axis of $R_\alpha, R_{\beta_1}, R_{\beta_2}, R_\gamma$, respectively. The rotation matrix OR ^[15,16] of the mechanism is expressed by YXY Euler angle

$${}^OR = \begin{bmatrix} -s\alpha c\beta s\gamma + c\alpha c\gamma & s\alpha s\beta & s\alpha c\beta c\gamma + c\alpha s\gamma \\ s\beta s\gamma & c\beta & -s\beta c\gamma \\ -c\alpha c\beta s\gamma - s\alpha c\gamma & c\alpha s\beta & c\alpha c\beta c\gamma - s\alpha s\gamma \end{bmatrix} \quad (1)$$

where $s=\sin$, $c=\cos$, $c\gamma=\frac{D \times c\alpha + 2z \times s\alpha - 2x \times c\alpha}{d}$.

Table 4 Feasible limbs and 5-DOF PMs

PM types	Evolutionary kinematic chains	Four kinematic chains	PMs
(a)	$\{xPyP^xR^xR/xPyP^xR^xR\}-yR$	SPS or UPS	4SPS+ $\{xPyP^xR^xR/xPyP^xR^xR\}-yR$
	$\{xP^zP^xR^xR/xP^zP^xR^xR\}-yR$		4SPS+ $\{xP^zP^xR^xR/xP^zP^xR^xR\}-yR$
	$\{xPyP^zP^xR/xPyP^zP^xR\}-yR$		4SPS+ $\{xPyP^zP^xR/xPyP^zP^xR\}-yR$
	$\{xC^xR^xR/xC^xR^xR\}-yR$		4SPS+ $\{xC^xR^xR/xC^xR^xR\}-yR$
	$\{xCyP^xR/xCyP^xR\}-yR$		4SPS+ $\{xCyP^xR/xCyP^xR\}-yR$
	$\{xC^zP^xR/xC^zP^xR\}-yR$		4SPS+ $\{xC^zP^xR/xC^zP^xR\}-yR$
	$\{xC^zPyP/xC^zPyP\}-yR$		4SPS+ $\{xC^zPyP/xC^zPyP\}-yR$
(b)	$\{yP^zP^xC/xR^zP^xC\}-yR$	SPS or UPS	4SPS+ $\{yP^zP^xC/xR^zP^xC\}-yR$
	$\{xR^yR^xC/xR^yR^xC\}-yR$		4SPS+ $\{xR^yR^xC/xR^yR^xC\}-yR$
	$\{xR^yP^xC/xR^yP^xC\}-yR$		4SPS+ $\{xR^yP^xC/xR^yP^xC\}-yR$
	$\{yP^zP^xC/yP^zP^xC\}-yR$		4SPS+ $\{yP^zP^xC/yP^zP^xC\}-yR$
	$\{xR^yP^xR^xP/xR^yP^xR^xP\}-yR$		4SPS+ $\{xR^yP^xR^xP/xR^yP^xR^xP\}-yR$
	$\{xR^zP^xR^xP/xR^zP^xR^xP\}-yR$		4SPS+ $\{xR^zP^xR^xP/xR^zP^xR^xP\}-yR$
	$\{xR^yP^zP^xP/xR^yP^zP^xP\}-yR$		4SPS+ $\{xR^yP^zP^xP/xR^yP^zP^xP\}-yR$
(c)	$\{yU^xxR^xR/yU^xxR^xR\}-yR$	SPS or UPS	4SPS+ $\{yU^xxR^xR/yU^xxR^xR\}-yR$
	$\{yU^xzP^xR/yU^xzP^xR\}-yR$		4SPS+ $\{yU^xzP^xR/yU^xzP^xR\}-yR$
	$\{yU^xyP^xR/yU^xyP^xR\}-yR$		4SPS+ $\{yU^xyP^xR/yU^xyP^xR\}-yR$
	$\{yU^xzPyP/yU^xzPyP\}-yR$		4SPS+ $\{yU^xzPyP/yU^xzPyP\}-yR$
	$\{yU^xyP^xR/yU^xyP^xR\}-yR$		4SPS+ $\{yU^xyP^xR/yU^xyP^xR\}-yR$
	$\{yC^xxR^xR/yC^xxR^xR\}-yR$		4SPS+ $\{yC^xxR^xR/yC^xxR^xR\}-yR$
	$\{yC^xzP^xR/yC^xzP^xR\}-yR$		4SPS+ $\{yC^xzP^xR/yC^xzP^xR\}-yR$
(d)	$\{yP^xR^xR^yR/yP^xR^xR^yR\}-yR$	SPS or UPS	4SPS+ $\{yP^xR^xR^yR/yP^xR^xR^yR\}-yR$
	$\{zP^xR^xR^yR/zP^xR^xR^yR\}-yR$		4SPS+ $\{zP^xR^xR^yR/zP^xR^xR^yR\}-yR$
	$\{yP^zP^xR^yR/yP^zP^xR^yR\}-yR$		4SPS+ $\{yP^zP^xR^yR/yP^zP^xR^yR\}-yR$
	$\{yP^xR^xUy/yP^xR^xUy\}-yR$		4SPS+ $\{yP^xR^xUy/yP^xR^xUy\}-yR$
	$\{zP^xR^xUy/zP^xR^xUy\}-yR$		4SPS+ $\{zP^xR^xUy/zP^xR^xUy\}-yR$
	$\{zPyP^xUy/zPyP^xUy\}-yR$		4SPS+ $\{zPyP^xUy/zPyP^xUy\}-yR$
	$\{xR^xR^xUy/xR^xR^xUy\}-yR$		4SPS+ $\{xR^xR^xUy/xR^xR^xUy\}-yR$
	$\{zP^xR^yC/zP^xR^yC\}-yR$		4SPS+ $\{zP^xR^yC/zP^xR^yC\}-yR$
	$\{xR^xR^yC/xR^xR^yC\}-yR$		4SPS+ $\{xR^xR^yC/xR^xR^yC\}-yR$
	$\{zP^xR^yC/zP^xR^yC\}-yR$		4SPS+ $\{zP^xR^yC/zP^xR^yC\}-yR$

The coordinates of A_i and B_i can be expressed in Table 5, $i=1, \dots, 6$. The coordinates of B_i in O -XYZ are expressed as

$${}^OB_i = {}^OO + {}^OR - {}^OB_i \quad (2)$$

where OB_i is a description of B_i in o -uvw, OB_i is a description of B_i in O -XYZ.

The length vector of the kinematic chain of the mechanism in O -XYZ is expressed as

$$l_i = {}^OA_i - {}^OB_i \quad (3)$$

where OA_i is the description of A_i in O -XYZ, l_i is vector length of the chain i .

The displacement of the actuated joint of the mechanism is expressed as

$$S_i = l_i - l_{i0} \quad (4)$$

where S_i is the variable length of the chain i .

The OoB_iA_i closed-loop constraint equation in O -XYZ is written as

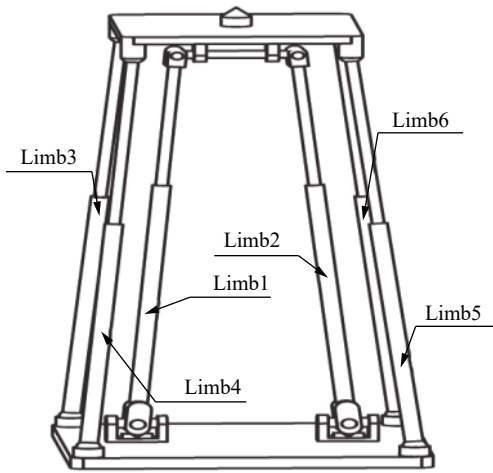


Fig. 3 3D model of 4SPS-(2UPR)R

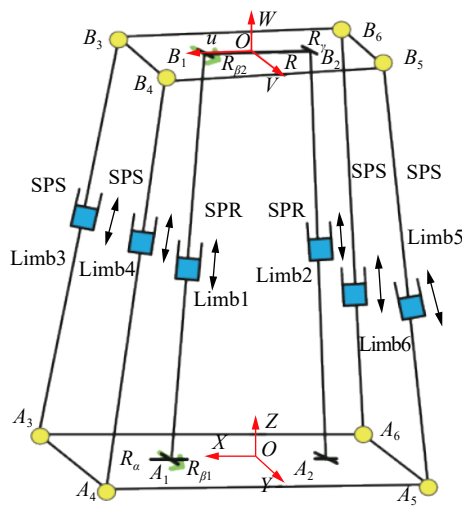


Fig. 4 Schematic of the mechanism

$$Oo + oB_i = OA_i + A_iB_i \quad (5)$$

where $Oo = {}^Oo$, $B_i o = -{}^Oo R^o B_i$, OA_i is the vector length of O to A_i , A_iB_i is the vector length of A_i to B_i .

$$A_iB_i = l_i = q_i w_i \quad (6)$$

where q_i is the length of the chain i , w_i is unit vector direction of the chain i .

The equation of each kinematic chain based on (5) and Oo is written as

$$\begin{cases} q_i = |{}^Oo + oB_i - OA_i| \\ w_i = \frac{{}^Oo + oB_i - OA_i}{q_i} \end{cases}, \quad i = 1, \dots, 6. \quad (7)$$

3.3 Velocity analysis

In order to establish a relationship between output ve-

locity of the o point and velocity of the P actuated joint, (5) is differentiated by time and the velocity of B_i is written as

$$v_{B_i} = v + \omega \times ({}^Oo R \cdot {}^oB_i) = \dot{q}_i w_i + q_i \omega_i \times w_i \quad (8)$$

where v is the linear velocity of o , ω is angular velocity of o , ω_i is angular velocity of the kinematic chain i , \dot{q}_i is velocity of the P actuated joint.

Multiply w_i on both sides of (8), (8) is separately obtained because of $w_i^T(\omega_i \times w_i) = 0$.

$$w_i^T v + ({}^Oo R \cdot {}^oB_i \times w_i)^T \omega = \dot{q}_i, \quad (i = 1, \dots, 6). \quad (9)$$

Equation (9) is written as

$$\dot{q}_i = \begin{bmatrix} w_i^T ({}^Oo R \cdot {}^oB_i \times w_i)^T \end{bmatrix} \begin{bmatrix} v \\ \omega \end{bmatrix} = J_{qi} \begin{bmatrix} v \\ \omega \end{bmatrix} = J_{qi} v_s \quad (10)$$

where J_{qi} is the Jacobi matrix of the actuated mechanism.

Equation (10) is the relation between velocity of P actuated joint and output velocity of the moving platform. Translational velocity of the moving platform in the Cartesian coordinates system is coincident as translational velocity in a generalized coordinate system. But the rotational velocity of the moving platform in the Cartesian coordinates system is different from the rotational velocity in the generalized coordinate system.

The rotational velocity of the moving platform can be expressed by the derivative of the Euler angle.

$$\begin{aligned} \omega &= R(X, \alpha) \begin{bmatrix} 1 \\ 0 \\ 0 \end{bmatrix} \dot{\alpha} + R(X, \alpha) R(Y, \beta) \begin{bmatrix} 0 \\ 1 \\ 0 \end{bmatrix} \dot{\beta} + \\ &R(X, \alpha) \times R(Y, \beta) R(Z, \gamma) \begin{bmatrix} 0 \\ 0 \\ 1 \end{bmatrix} \dot{\gamma} = \\ &\begin{bmatrix} 1 & 0 & \sin \beta \\ 0 & \cos \alpha & -\sin \alpha \\ 0 & \sin \alpha & \cos \alpha \cos \beta \end{bmatrix} \begin{bmatrix} \dot{\alpha} \\ \dot{\beta} \\ \dot{\gamma} \end{bmatrix}. \end{aligned} \quad (11)$$

Equation (11) is represented as

$$\omega = \begin{bmatrix} 1 & 0 & \sin \beta \\ 0 & \cos \alpha & -\sin \alpha \\ 0 & \sin \alpha & \cos \alpha \cos \beta \end{bmatrix} \begin{bmatrix} \dot{\alpha} \\ \dot{\beta} \\ \dot{\gamma} \end{bmatrix} = J_\omega v_s \quad (12)$$

when the mechanism is 3t2r, the six-dimensional velocity of the moving platform is represented as

$$\begin{bmatrix} v \\ \omega \end{bmatrix} = J_{01} \begin{bmatrix} v \\ \dot{\alpha} \\ \dot{\beta} \end{bmatrix} \quad (13)$$

$$\text{where } J_{01} = \begin{bmatrix} 1 & 0 & 0 & 0 & 0 \\ 0 & 1 & 0 & 0 & 0 \\ 0 & 0 & 1 & 0 & 0 \\ 0 & 0 & 0 & 1 & 0 \\ 0 & 0 & 0 & 0 & c_\alpha \\ 0 & 0 & 0 & 0 & s_\alpha \end{bmatrix}.$$

When the mechanism is 2t3r, the mechanism does not have Y translation. The six-dimensional velocity of the moving platform is represented as

$$\begin{bmatrix} v \\ \omega \end{bmatrix} = J_{02} \begin{bmatrix} \dot{X} \\ \dot{Z} \\ \omega \end{bmatrix} \quad (14)$$

$$\text{where } J_{02} = \begin{bmatrix} 1 & 0 & 0 & 0 & 0 & 0 \\ 0 & 0 & 0 & 0 & 0 & 0 \\ 0 & 0 & 1 & 0 & 0 & 0 \\ 0 & 0 & 0 & 1 & 0 & \sin \beta \\ 0 & 0 & 0 & 0 & \cos \alpha & -\sin \alpha \\ 0 & 0 & 0 & 0 & \sin \alpha & \cos \alpha \cos \beta \end{bmatrix}.$$

The Jacobi matrix between the velocity of the P joint and output independent parameter velocity of the mechanism is written as

$$J = J_{qi} J_0 \quad (15)$$

where J_0 is J_{01} or J_{02} .

The angular velocity of the kinematic chain i is obtained by (8) which crosses w_i on both sides,

$$\omega_i = \frac{w_i \times v_{Bi}}{q_i} = J_{wi} \begin{bmatrix} v \\ \omega \end{bmatrix}. \quad (16)$$

The linear velocity of B_i is written as

$$v_{Bi} = v + \omega \times ({}^O R \cdot {}^O B_i) = \begin{bmatrix} I_{3 \times 3} & -S(B_i) \end{bmatrix} \begin{bmatrix} v \\ \omega \end{bmatrix} = J_{ri} \begin{bmatrix} v \\ \omega \end{bmatrix} \quad (17)$$

$$\text{where } J_{ri} = \begin{bmatrix} I_{3 \times 3} & -S(B_i) \end{bmatrix}.$$

The Jacobi matrix of the angular velocity of the kinematic chain i is written as

$$J_{wi} = \frac{S(w_i)}{q_i} J_{ri} \quad (18)$$

where $S(w_i)$ and $S(B_i)$ are anti-symmetric matrices.

$$S(w_i) = \begin{bmatrix} 0 & -w_{iz} & w_{iy} \\ w_{iz} & 0 & -w_{ix} \\ -w_{iy} & w_{ix} & 0 \end{bmatrix}$$

$$S(B_i) = \begin{bmatrix} 0 & -B_{iz} & B_{iy} \\ B_{iz} & 0 & -B_{ix} \\ -B_{iy} & B_{ix} & 0 \end{bmatrix}.$$

The kinematic chain i includes the oscillating rod and telescopic rod in Fig. 5, all oscillating rod and telescopic rods connect the fixed platform with the moving platform. The mass center of the oscillating rod is M_{Ai} , the distance from M_{Ai} to S_i of fixed platform is l_{1Si} . The mass center of the telescopic rod is M_{Bi} , the distance from M_{Bi} to the S_i of the moving platform is l_{2Si} .

The linear velocity of M_{Ai} is written as

$$v_{MAi} = l_{1Si} \omega_i \times w_i = -l_{1Si} S(w_i) J_{wi} \begin{bmatrix} v \\ \omega \end{bmatrix} = J_{vAi} \begin{bmatrix} v \\ \omega \end{bmatrix} \quad (19)$$

where $J_{vAi} = -l_{1Si} S(w_i) J_{wi}$.

The linear velocity of M_{Bi} is written as

$$v_{MBi} = \dot{w}_i q_i + (l_i - l_{2Si}) \omega_i \times w_i = J_{vBi} \begin{bmatrix} v \\ \omega \end{bmatrix} \quad (20)$$

where

$$J_{vBi} = \left[I + \frac{l_{2Si}}{q_i} S(w_i)^2 - \left(S(B_i) + \frac{l_{2Si} S(w_i)^2 S(B_i)}{q_i} \right) \right].$$

Angular velocities of the oscillating rod and telescopic rod are the same and can be written as

$$\omega_i = \frac{w_i \times v_{Bi}}{q_i} = J_{wi} \begin{bmatrix} v \\ \omega \end{bmatrix}. \quad (21)$$

Jacobi matrices of the velocity of the oscillating rod and telescopic rod are written as

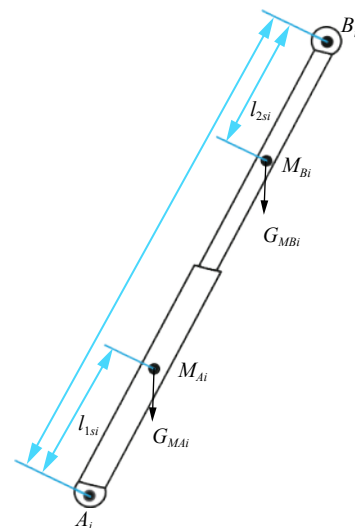


Fig. 5 Schematic of the chain

$$J_{v\omega Ai} = \begin{bmatrix} J_{vAi} \\ J_{wi} \end{bmatrix}, \quad J_{v\omega Bi} = \begin{bmatrix} J_{vBi} \\ J_{wi} \end{bmatrix}.$$

3.4 Acceleration analysis

Equation (5) is differentiated by time, the acceleration of B_i is obtained.

$$\dot{v}_{Bi} = \dot{v} + \dot{\omega} \times (R \cdot {}^o B_i) + \omega \times (\omega \times (R \cdot {}^o B_i)). \quad (22)$$

$$\begin{aligned} \dot{v}_{Bi} = & \ddot{q}_i w_i + \dot{q}_i \omega_i \times w_i + \dot{q}_i \omega_i \times w_i + \\ & q_i \dot{\omega}_i \times w_i + q_i \omega_i \times (\omega_i \times w_i). \end{aligned} \quad (23)$$

Dot product both sides of (23) by w_i , the angular acceleration of P joint is obtained

$$\dot{\omega}_i = \frac{w_i \times \dot{v}_{Bi} - 2\dot{q}_i \omega_i}{q_i} = J_{wi} \begin{bmatrix} a & \varepsilon \end{bmatrix}^T + K_{wi} \begin{bmatrix} v & \omega \end{bmatrix}^T \quad (24)$$

$$\text{where } K_{wi} = \frac{S(w_i) \dot{J}_{ri} - 2J_{qi} J_{wi} [v \quad \omega]^T}{q_i}.$$

Equation (8) multiplying w_i is additionally written as

$$\dot{q}_i = w_i^T \cdot v_{Bi}. \quad (25)$$

Equation (25) is differentiated by time. The linear acceleration of the P joint is obtained as

$$\dot{q}_i = w_i^T \dot{v}_{Bi} + v_{Bi}^T (\omega_i \times w_i) = J_{qi} [a \quad \varepsilon]^T + K_{li} [v \quad \omega]^T \quad (26)$$

$$\text{where } K_{li} = w_i^T \times J_r - [J_r [vw]^T]^T \times S(w_i) J_{wi}.$$

Because $\dot{\omega}_i$ and ω_i are known, linear acceleration of the oscillating rod is additionally written as

$$\begin{aligned} \dot{v}_{MAi} = & l_{1Si} \dot{\omega}_i \times w_i + l_{1Si} \omega_i \times (\omega_i \times w_i) = \\ & J_{vAi} \begin{bmatrix} a & \varepsilon \end{bmatrix}^T + J_{Ai} \begin{bmatrix} v & \omega \end{bmatrix}^T \end{aligned} \quad (27)$$

$$\text{where } J_{Ai} = -l_{1Si} S(w_i) K_{wi} - l_{1Si} w_i \times (J_{wi} [v \quad \omega]^T)^T J_{wi}.$$

Linear acceleration of the telescopic rod is additionally written as

$$\begin{aligned} \dot{v}_{MBi} = & \ddot{q}_i w_i + 2\dot{q}_i (\omega_i \times w_i) + (l_i - l_{2Si}) \dot{\omega}_i \times w_i + \\ & (l_i - l_{2Si}) \omega_i \times (\omega_i \times w_i) = J_{vBi} \begin{bmatrix} a & \varepsilon \end{bmatrix} + J_{Bi} \begin{bmatrix} v & \omega \end{bmatrix} \end{aligned} \quad (28)$$

where

$$\begin{aligned} J_{Bi} = & w_i K_{li} - 2J_{qi} [v \quad \omega] S(w_i) J_{wi} + \\ & (l_{2Si} - l) [S(w_i) K_{wi} + w_i (J_{wi} [v \quad \omega]^T)^T J_{wi}]. \end{aligned}$$

4 Dynamics analysis

4.1 Force analysis of the mechanism

The gravity of the kinematic chain i is G_{mi} , the inertia force and inertia moment of the kinematic chain i are f_{mi} and T_{mi} , respectively. Gravities of the fixed platform and moving platform are G_O and G_o , respectively. External force and the external torque of the moving platform are 0, respectively. The masses of the kinematic chain, the fixed platform and the moving platform are m_{mi} , m_O and m_o , respectively.

$$\begin{cases} G_{mi} = m_{mi}g \\ f_{mi} = -m_{mi}a_{mi} \\ G_O = m_Og \\ G_o = m_o g. \end{cases} \quad (29)$$

The inertial force and inertial moment of the moving platform in O -XYZ can be written as

$$\begin{bmatrix} f_o \\ T_o \end{bmatrix} = \begin{bmatrix} -m_o a \\ -{}^O I_o \varepsilon - \omega \times ({}^O I_o \omega) \end{bmatrix} \quad (30)$$

where ${}^O I_o$ is the inertia matrix of the moving platform in O -XYZ.

The inertial force and inertial moment of the oscillating rod of the kinematic chain i in O -XYZ can be written as

$$\begin{bmatrix} f_{MAi} \\ T_{MAi} \end{bmatrix} = \begin{bmatrix} -m_{MAi} a \\ -{}^O I_{MAi} \varepsilon - \omega \times ({}^O I_{MAi} \omega) \end{bmatrix} \quad (31)$$

where ${}^O I_{MAi}$ is the inertia matrix of the oscillating rod in O -XYZ, m_{MAi} is mass of the oscillating rod of the kinematic chain i in O -XYZ.

The inertial force and the inertial moment of the telescopic rod of the kinematic chain i in O -XYZ can be written as

$$\begin{bmatrix} f_{MBi} \\ T_{MBi} \end{bmatrix} = \begin{bmatrix} -m_{MBi} a \\ -{}^O I_{MBi} \varepsilon - \omega \times ({}^O I_{MBi} \omega) \end{bmatrix} \quad (32)$$

where ${}^O I_{MBi}$ is the inertia matrix of the telescopic rod in O -XYZ, m_{MBi} is mass of the telescopic rod of the kinematic chain i in O -XYZ.

${}^O I_{MBi}$, ${}^O I_{MAi}$ and ${}^O I_o$ can be written as

$$\begin{cases} {}^O I_o = {}^O R {}^o I_o ({}^O R)^T \\ {}^O I_{MAi} = {}^O R_i {}^i I_{Ai} ({}^O R_i)^T \\ {}^O I_{MBi} = {}^O R_i {}^i I_{Bi} ({}^O R_i)^T \end{cases} \quad (33)$$

where oI_o is the inertial matrix of the moving platform in $o-uvw$, oR_i is the inertial matrix of the kinematic chain i in $O-XYZ$, ${}^iI_{Ai}$ is the inertial matrix of the telescopic rod in the chain local coordinate system and ${}^iI_{Bi}$ is the inertial matrix of the oscillating rod in the chain local coordinate system.

4.2 Establishment of dynamic model

When the mechanism is under no-load, the force and moment of the moving platform in $O-XYZ$ are written as

$$F_o = \begin{bmatrix} G_o - f_o \\ T_o \end{bmatrix} = \begin{bmatrix} m_o g - m_o a \\ -{}^O I_o \varepsilon - \omega \times ({}^O I_o \omega) \end{bmatrix}. \quad (34)$$

The force and moment of the telescopic rod of the kinematic chain i in $O-XYZ$ are written as

$$F_{MBi} = \begin{bmatrix} G_{mBi} + f_{MBi} \\ T_{MBi} \end{bmatrix} = \begin{bmatrix} m_{MBi} g - m_{MBi} a_B \\ -{}^O I_{MBi} \varepsilon_B - \omega_i \times ({}^O I_{MBi} \omega_i) \end{bmatrix}. \quad (35)$$

The force and moment of the oscillating rod of the kinematic chain i in $O-XYZ$ are written as

$$F_{MAi} = \begin{bmatrix} G_{mAi} + f_{MAi} \\ T_{MAi} \end{bmatrix} = \begin{bmatrix} m_{MAi} g - m_{MAi} a_A \\ -{}^O I_{MAi} \varepsilon_A - \omega_i \times ({}^O I_{MAi} \omega_i) \end{bmatrix}. \quad (36)$$

The dynamic equilibrium equation of the mechanism based on the principle of virtual work is obtained under ideal state.

$$v_i^T F + v_s^T F_o + \sum_i (v_{MAi}^T F_{MAi} + v_{MBi}^T F_{MBi}) = 0 \quad (37)$$

where F is actuated force, $v_i = Jv_s = J_q J_o v_s$, $v_{MAi} = J_{v\omega Ai} v_s$, $v_{MBi} = J_{v\omega Bi} v_s$.

Equation (37) can also be written as

$$(J_q^T F + F_o + \sum_i J_{v\omega Ai}^T F_{MAi} + \sum_i J_{v\omega Bi}^T F_{MBi}) = 0 \quad (37a)$$

$$F = -[J_o^T J_q^T]^+ J_o^T \times \left(F_o + \sum_i J_{v\omega Ai}^T F_{MAi} + \sum_i J_{v\omega Bi}^T F_{MBi} \right). \quad (37b)$$

Equation (37b) can also be written as

$$F = M\ddot{q} + C\dot{q} + G - [J_o^T J_q^T]^+ J_o^T \begin{bmatrix} F_o \\ T_o \end{bmatrix} \quad (37c)$$

where M is the inertia matrix, G is the gravity matrix, C is the velocity matrix.

$$\begin{aligned} M &= [J_o^T J_q^T]^+ J_o^T \left\{ \begin{bmatrix} m_o J_v & o \\ o & I_o J_\omega \end{bmatrix} + \right. \\ &\quad \sum_i J_{v\omega Ai}^T \begin{bmatrix} m_{MAi} J_{vAi} & o \\ o & I_{MAi} J_{\omega i} \end{bmatrix} + \\ &\quad \left. \sum_i J_{v\omega Bi}^T \begin{bmatrix} m_{MBi} J_{vBi} & o \\ o & I_{MBi} J_{\omega i} \end{bmatrix} \right\} \\ C &= [J_o^T J_q^T]^+ J_o^T \left\{ \begin{bmatrix} 0 \\ \omega \times I_\omega \end{bmatrix} + \sum_i J_{v\omega Ai}^T \begin{bmatrix} 0 \\ \omega_i \times (I_{MAi} \omega_i) \end{bmatrix} + \right. \\ &\quad \left. \sum_i J_{v\omega Bi}^T \begin{bmatrix} 0 \\ \omega_i \times (I_{MBi} \omega_i) \end{bmatrix} \right\} \\ G &= -[J_o^T J_q^T]^+ J_o^T \left\{ \begin{bmatrix} m_o g \\ 0 \end{bmatrix} + \sum_i J_{v\omega Ai}^T \begin{bmatrix} m_{MAi} g \\ 0 \end{bmatrix} + \right. \\ &\quad \left. \sum_i J_{v\omega Bi}^T \begin{bmatrix} m_{MBi} g \\ 0 \end{bmatrix} \right\}. \end{aligned}$$

4.3 Verification of dynamic mathematical model of the mechanism

The structural parameters of the redundantly actuated parallel mechanism are given in Table 5. The motion trajectory of o is circular motion in the XY plane. The motion trajectory equation of o is given as

$$\begin{cases} X = 0.05 \cos(2t) \\ Y = -0.05 \sin(2t) \\ Z = 1.2 \text{ m} \\ \alpha = 0^\circ \\ \beta = 0^\circ. \end{cases} \quad (38)$$

The actuated force of the six actuated joints of the mechanism under a no-load operation can be obtained. Fig. 6 shows the theoretical result of the actuated force. The change rule of the six actuated forces of six kinematic chains is sine or cosine. The actuated forces of the Chain 1 and Chain 2 are bigger than the other four chains. F_3 and F_6 , F_1 and F_2 , F_4 and F_5 are equal in size when the mechanism is in the initial position, respectively. F_3 and F_4 , F_1 and F_2 , F_5 and F_6 are symmetrical and differ by one cycle, respectively. Fig. 7 shows the simulation result of the actuated force. Theoretical results by Matlab are

Table 5 Structural and physical parameters

Parameters	Descriptions	Values	Units
D	Radius of the fixed platform	1	m
d	Radius of the moving platform	0.5	m
A_1	Coordinate of A_1 in O -XYZ	$(\frac{D}{2}, 0, 0)$	m
A_2	Coordinate of A_2 in O -XYZ	$(-\frac{D}{2}, 0, 0)$	m
A_3	Coordinate of A_3 in O -XYZ	$(D \frac{\sqrt{2}}{2}, D \frac{\sqrt{2}}{2}, 0)$	m
A_4	Coordinate of A_4 in O -XYZ	$(D \frac{\sqrt{2}}{2}, -D \frac{\sqrt{2}}{2}, 0)$	m
A_5	Coordinate of A_5 in O -XYZ	$(-D \frac{\sqrt{2}}{2}, -D \frac{\sqrt{2}}{2}, 0)$	m
A_6	Coordinate of A_6 in O -XYZ	$(-D \frac{\sqrt{2}}{2}, D \frac{\sqrt{2}}{2}, 0)$	m
B_1	Coordinate of B_1 in o -uvw	$(\frac{d}{2}, 0, 0)$	m
B_2	Coordinate of B_2 in o -uvw	$(-\frac{d}{2}, 0, 0)$	m
B_3	Coordinate of B_3 in o -uvw	$(d \frac{\sqrt{2}}{2}, d \frac{\sqrt{2}}{2}, 0)$	m
B_4	Coordinate of B_4 in o -uvw	$(d \frac{\sqrt{2}}{2}, -d \frac{\sqrt{2}}{2}, 0)$	m
B_5	Coordinate of B_5 in o -uvw	$(-d \frac{\sqrt{2}}{2}, -d \frac{\sqrt{2}}{2}, 0)$	m
B_6	Coordinate of B_6 in o -uvw	$(-d \frac{\sqrt{2}}{2}, d \frac{\sqrt{2}}{2}, 0)$	m
l_{1Si}	Length of l_{1Si}	0.5	m
l_{2Si}	Length of l_{2Si}	0.5	m
I_{MBi}	Inertia matrix of the telescopic rod	diag(0.017, 0.000 471, 0.376)	kg·m ²
I_{MAi}	Inertia matrix of the oscillating rod	diag(0.02, 0.000 838, 0.019)	kg·m ²
I_o	Inertia matrix of the moving platform	diag(0.378, 0.746, 0.376)	kg·m ²
g	Gravitational acceleration	[0 0 -9.807] ^T	m/s ²
m_{MBi}	Mass of the telescopic rod	1.14	kg
m_{MAi}	Mass of the oscillating rod	1.3	kg
m_o	Mass of the moving platform	2.8	kg
t	Timing of the mechanism's movements	4	s

basically consistent with simulation results by ADAMS. The dynamic mathematical model of the 4SPS-(2UPR)R parallel mechanism is shown to be correct by Matlab and ADAMS under no-load conditions. So the simulation results and theoretical results are consistent with the described mechanism.

5 Dynamics performance evaluation analysis of the mechanism

5.1 Acceleration performance analysis of the mechanism

The dynamic acceleration performance index can evaluate the acceleration and deceleration characteristics of the mechanism. In (37c), the inertia factor mainly affects

the acceleration and deceleration characteristics, the latter three terms are not considered. Equation (37c) is simplistically obtained as

$$F \approx M\ddot{q} \quad (39)$$

where

$$M = [J_o^T J_q^T]^+ \left\{ J_o^T \begin{bmatrix} m_o E & o \\ o & I_o \end{bmatrix} J_o + \sum_i J_o^T J_{v\omega Ai}^T \begin{bmatrix} m_{MAi} E & o \\ o & I_{MAi} \end{bmatrix} J_{v\omega Ai} J_o + \sum_i J_o^T J_{v\omega Bi}^T \begin{bmatrix} m_{MBi} E & o \\ o & I_{MBi} \end{bmatrix} J_{v\omega Bi} J_o \right\}$$

Equation (39) can also be written as

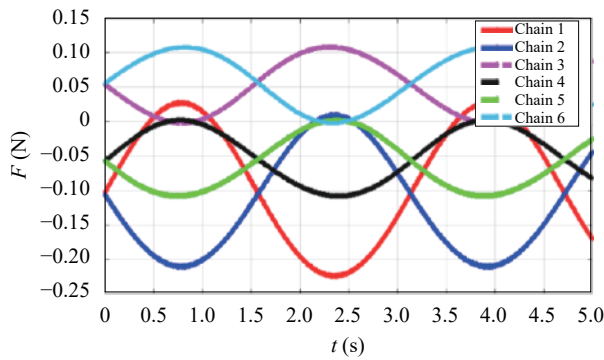


Fig. 6 Theoretical value of the mechanism. Colored figures are available in the online version.

$$\ddot{q} \approx [M]^+ F \quad (40)$$

where $[M]^+$ is the generalized pseudo-inverse matrix of M .

At present, the acceleration performance evaluation index can take advantage of the harmonic average harmonic mean (HMIM)^[31] as the dynamic performance evaluation index in (41). The value of HMIM will be larger when both the maximum singular value and the minimum singular value are larger. To ensure that the mechanism has good isotropy and achieve good acceleration performance, the value of HMIM of the mechanism should be getting bigger and be expressed as

$$\eta_{HMIM} = \frac{2}{\frac{1}{\sigma_{\max}} + \frac{1}{\sigma_{\min}}} \quad (41)$$

where σ_{\max} and σ_{\min} are the maximum and minimum singular values of $[M]^+$, respectively.

Because the mechanism has translation and rotation, its dimension is not uniform, translational acceleration performance and rotational acceleration performance should be analyzed, respectively.

Fig. 8 shows the translational acceleration performance of the mechanism from different views. The translational acceleration performance of the mechanism is approximately symmetric along the X -axis and Y -axis, respectively. The mechanism has the best translational acceleration performance in Chain 1 or Chain 2 local vicinity, respectively.

Fig. 9 shows the rotational acceleration performance of the mechanism from different views. The mechanism has the best rotational acceleration performance in the middle of the Chain 1 and Chain 2. Compared with [31], the numerical results of HMIM are relatively large in Figs. 8 and 9. The results show that the mechanism has good acceleration performance.

5.2 Isotropic evaluation based on energy transfer efficiency

Because the mechanism has translation and rotation,

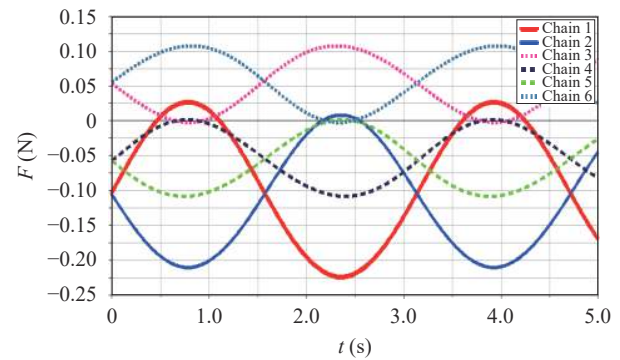


Fig. 7 Simulation value of the mechanism

its dimension is not uniform. The energy transfer efficiency^[32] can be used to avoid dimensional inconsistency of the mechanism and evaluate dynamic performance.

The kinetic energy of the moving platform is expressed as

$$E_o = \frac{1}{2} m_o v^2 + \frac{1}{2} I_o \omega^2 = \frac{1}{2} \begin{bmatrix} v \\ \omega \end{bmatrix}^T \begin{bmatrix} m_o E & 0 \\ 0 & I_o \end{bmatrix} \begin{bmatrix} v \\ \omega \end{bmatrix}. \quad (42)$$

The oscillating rod only has rotational motion, and the kinetic energy of the oscillating rod i is expressed as

$$E_{Ai} = \frac{1}{2} I_i \omega_i^2 = \frac{1}{2} \begin{bmatrix} v \\ \omega \end{bmatrix}^T J_{v\omega A}^T \begin{bmatrix} o & o \\ o & I_{MAi} \end{bmatrix} J_{v\omega A} \begin{bmatrix} v \\ \omega \end{bmatrix}. \quad (43)$$

Each telescopic rod has both translation and rotation motion, and the kinetic energy of the telescopic rod i is expressed as

$$E_{Bi} = \frac{1}{2} m_{Bi} v_{mBi}^2 + \frac{1}{2} I_i \omega_i^2 = \frac{1}{2} \begin{bmatrix} v_{mBi} \\ \omega_i \end{bmatrix}^T \begin{bmatrix} m_{Bi} E & 0 \\ 0 & I_i \end{bmatrix} \begin{bmatrix} v_{mBi} \\ \omega_i \end{bmatrix} = \frac{1}{2} \begin{bmatrix} v \\ \omega \end{bmatrix}^T J_{v\omega B}^T \begin{bmatrix} m_{Bi} E & o \\ o & I_{MBi} \end{bmatrix} J_{v\omega B} \begin{bmatrix} v \\ \omega \end{bmatrix}. \quad (44)$$

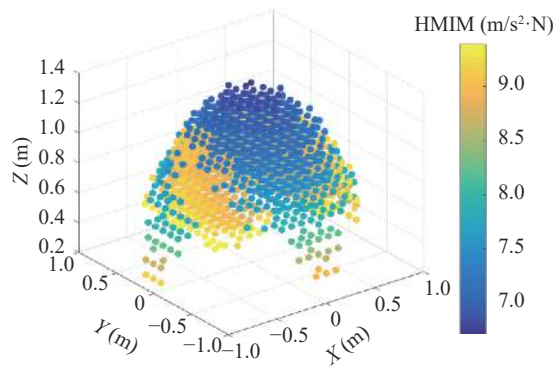
The total kinetic energy of the mechanism is expressed as

$$E_{all} = E_o + E_{Ai} + E_{Bi}. \quad (45)$$

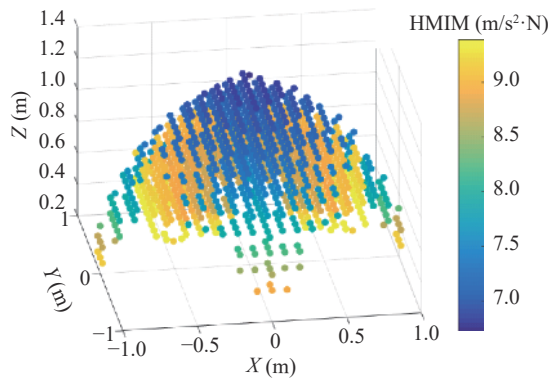
The energy proportion of the moving platform in the mechanism is expressed as

$$\eta_{KE} = \frac{E_o}{E_{all}} \times 100\%. \quad (46)$$

The kinetic energy of the moving platform is con-



(a) 45° angles of rotational acceleration performance



(b) 30° angles of rotational acceleration performance

Fig. 8 Different angles of translational acceleration performance

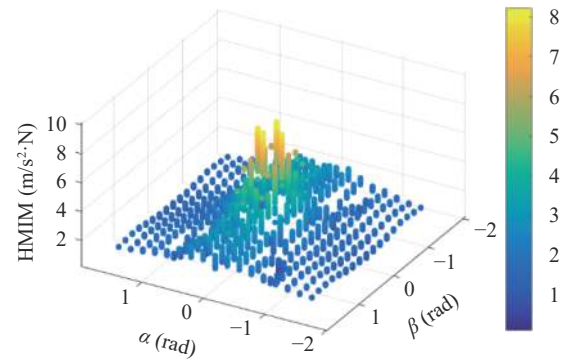
sidered as the effective energy of the mechanism, η_{KE} represents efficiency of the mechanism

Combined (42)–(46), η_{KE} is expressed as (47).

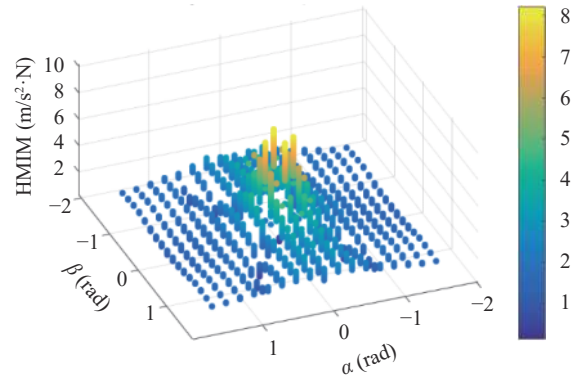
Fig. 10 shows the energy transfer efficiency of the mechanism from different views. The energy transfer efficiency of the mechanism is approximately symmetric along the X -axis and Y -axis, respectively. The mechanism has high energy transfer efficiency. The energy transfer efficiency of the mechanism is the best in the initial central position. Compared with [33], the numerical results of η_{KE} are relatively large in Fig. 10. The results show that the mechanism has good energy transfer efficiency.

6 Conclusions

This paper focuses on type synthesis and dynamics performance evaluation of a family of 5-DOF redundantly actuated parallel mechanisms, which are suitable for the parallel machining heads of a machine tool. This



(a) 45° angles of rotational acceleration performance



(b) 30° angles of rotational acceleration performance

Fig. 9 Different angles of rotational acceleration performance

paper mainly includes three aspects: 1) This paper presents a 5-DOF redundantly actuated parallel mechanism on the basis of Lie group theory and a configuration evolution method for the parallel machining head of the machine tool. This method is more intuitive and effective when the 5-DOF redundantly actuated parallel mechanism is designed. 2) A 4SPS-(2UPR)R mechanism suitable for the parallel machining head is selected. The kinematics and dynamics models of the parallel mechanism are established and verified to be correct by Matlab and ADAMS under no-load conditions. 3) By analyzing the translational acceleration, rotational acceleration performance and energy transfer efficiency of the mechanism, we find that 4SPS-(2UPR)R redundantly actuated parallel mechanism has not only good translational acceleration and rotational acceleration performance but also good energy transfer efficiency. This paper provides a practical parallel mechanism for the machining head of the machine tool, which will provide a foundation for control of the parallel mechanism.

$$\eta_{KE} = \frac{\frac{1}{2} \left(\begin{bmatrix} v \\ \omega \end{bmatrix}^T \begin{bmatrix} m_o & 0 \\ 0 & I_o \end{bmatrix} \begin{bmatrix} v \\ \omega \end{bmatrix} \right)}{\frac{1}{2} \begin{bmatrix} v \\ \omega \end{bmatrix}^T \begin{bmatrix} m_o & 0 \\ 0 & I_o \end{bmatrix} \begin{bmatrix} v \\ \omega \end{bmatrix} + \frac{1}{2} \begin{bmatrix} v \\ \omega \end{bmatrix}^T J_{v\omega A}^T \begin{bmatrix} 0 & 0 \\ 0 & I_o \end{bmatrix} J_{v\omega A} \begin{bmatrix} v \\ \omega \end{bmatrix} + \frac{1}{2} \begin{bmatrix} v \\ \omega \end{bmatrix}^T J_{v\omega B}^T \begin{bmatrix} m_{Bi} E & 0 \\ 0 & I_{MBi} \end{bmatrix} J_{v\omega B} \begin{bmatrix} v \\ \omega \end{bmatrix}} \times 100\%. \quad (47)$$

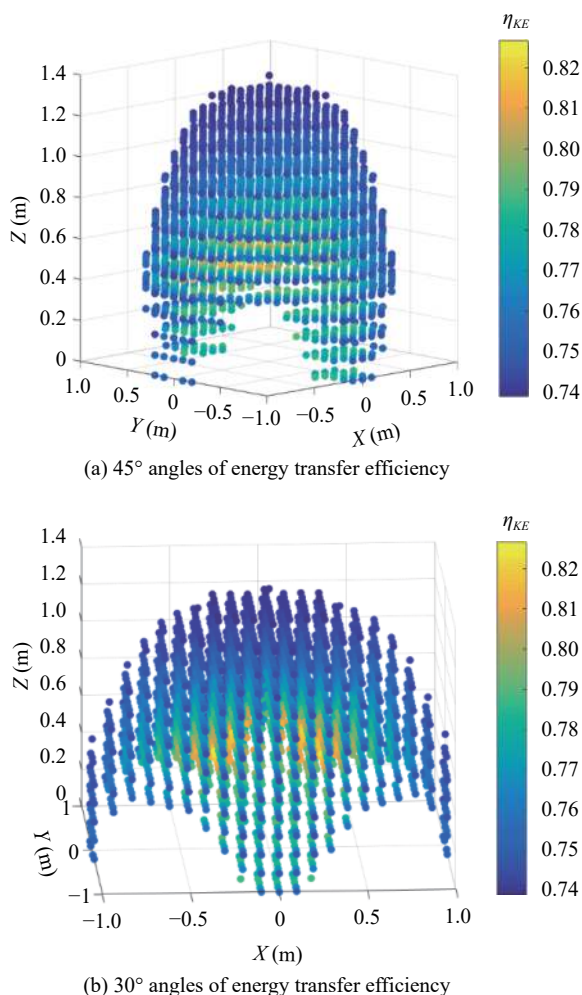


Fig. 10 Different angles of energy transfer efficiency

Acknowledgements

This work was supported by the Fundamental Research Funds for the Central Universities (No. 2018 JBZ007).

References

- [1] X. Chen, X. J. Liu, F. G. Xie, T. Sun. A comparison study on motion/force transmissibility of two typical 3-DOF parallel manipulators: The sprint Z3 and A3 tool heads. *International Journal of Advanced Robotic Systems*, vol. 11, no. 1, 2014. DOI: [10.5772/57458](https://doi.org/10.5772/57458).
- [2] J. Ghasemi, R. Moradinezhad, M. A. Hosseini. Kinematic synthesis of parallel manipulator via neural network approach. *International Journal of Engineering*, vol. 30, no. 9, pp. 1319–1325, 2017.
- [3] J. Zhang, Y. Q. Zhao, Y. Jin. Elastodynamic modeling and analysis for an Exechon parallel kinematic machine. *Journal of Manufacturing Science and Engineering*, vol. 138, no. 3, Article number 031011, 2016. DOI: [10.1115/1.4030938](https://doi.org/10.1115/1.4030938).
- [4] G. Han, F. G. Xie, X. J. Liu. Evaluation of the power consumption of a high-speed parallel robot. *Frontiers of Mechanical Engineering*, vol. 13, no. 2, pp. 167–178, 2018. DOI: [10.1007/s11465-017-0456-8](https://doi.org/10.1007/s11465-017-0456-8).
- [5] F. G. Xie, X. J. Liu. Analysis of the kinematic characteristics of a high-speed parallel robot with Schönflies motion: Mobility, kinematics, and singularity. *Frontiers of Mechanical Engineering*, vol. 11, no. 2, pp. 135–143, 2016. DOI: [10.1007/s11465-016-0389-7](https://doi.org/10.1007/s11465-016-0389-7).
- [6] Y. Wang, J. J. Yu, X. Pei. Fast forward kinematics algorithm for real-time and high-precision control of the 3-RPS parallel mechanism. *Frontiers of Mechanical Engineering*, vol. 13, no. 3, pp. 368–375, 2018. DOI: [10.1007/s11465-018-0519-5](https://doi.org/10.1007/s11465-018-0519-5).
- [7] W. D. Yu, H. Wang, G. L. Chen. Design and kinematic analysis of a 3-translational-DOF spatial parallel mechanism based on polyhedra. *Mechanism and Machine Theory*, vol. 121, pp. 92–115, 2018. DOI: [10.1016/j.mechmachtheory.2017.10.020](https://doi.org/10.1016/j.mechmachtheory.2017.10.020).
- [8] L. Jing, B. L. Liao, M. Liu, L. Xiao, D. S. Guo, X. G. Yan. Different-level simultaneous minimization scheme for fault tolerance of redundant manipulator aided with discrete-time recurrent neural network. *Frontiers in Neurorobotics*, vol. 11, Article number 50, 2017. DOI: [10.3389/fnbot.2017.00050](https://doi.org/10.3389/fnbot.2017.00050).
- [9] F. Prochazka, M. Valasek, Z. Sika. Robust sliding mode control of redundantly actuated parallel mechanisms with respect to geometric imperfections. *Multibody System Dynamics*, vol. 36, no. 3, pp. 221–236, 2016. DOI: [10.1007/s11044-015-9481-8](https://doi.org/10.1007/s11044-015-9481-8).
- [10] S. H. Wen, G. Q. Qin, B. W. Zhang, H. K. Lam, Y. S. Zhao, H. B. Wang. The study of model predictive control algorithm based on the force/position control scheme of the 5-DOF redundant actuation parallel robot. *Robotics and Autonomous Systems*, vol. 79, pp. 12–25, 2016. DOI: [10.1016/j.robot.2016.02.002](https://doi.org/10.1016/j.robot.2016.02.002).
- [11] D. Liang, Y. M. Song, T. Sun, X. Y. Jin. Rigid-flexible coupling dynamic modeling and investigation of a redundantly actuated parallel manipulator with multiple actuation modes. *Journal of Sound and Vibration*, vol. 403, pp. 129–151, 2017. DOI: [10.1016/j.jsv.2017.05.022](https://doi.org/10.1016/j.jsv.2017.05.022).
- [12] H. B. Qu. Type Synthesis and Parasitic Motion Avoidance of Redundantly Actuated Parallel Mechanisms, Ph.D. dissertation, Beijing Jiaotong University, China, 2013. (in Chinese)
- [13] X. L. Chen, D. Y. Jiang, L. L. Chen, Q. Wang. Kinematics performance analysis and optimal design of redundant actuation parallel mechanism. *Transactions of the Chinese Society for Agricultural Machinery*, vol. 47, no. 6, pp. 340–347, 2016. DOI: [10.6041/j.issn.1000-1298.2016.06.045](https://doi.org/10.6041/j.issn.1000-1298.2016.06.045). (in Chinese)
- [14] X. L. Chen, W. M. Feng, Y. S. Zhao. Dynamics model of 5-DOF parallel robot mechanism. *Transactions of the Chinese Society for Agricultural Machinery*, vol. 44, no. 1, pp. 236–243, 2013. DOI: [10.6041/j.issn.1000-1298.2013.01.044](https://doi.org/10.6041/j.issn.1000-1298.2013.01.044). (in Chinese)
- [15] Y. Lu, Y. Liu, L. J. Zhang, N. J. Ye, Y. L. Wang. Dynamics analysis of a novel 5-DoF parallel manipulator with couple-constrained wrench. *Robotica*, vol. 36, no. 10, pp. 1421–1435, 2018. DOI: [10.1017/S0263574718000474](https://doi.org/10.1017/S0263574718000474).
- [16] Y. Lu, Y. Liu, N. J. Ye. Dynamics analysis of a novel 5-DoF 3SPU+2SPRR type parallel manipulator. *Advanced Robotics*, vol. 30, no. 9, pp. 595–607, 2016. DOI: [10.1080/01691864.2015.1132637](https://doi.org/10.1080/01691864.2015.1132637).
- [17] J. T. Yao, W. D. Gu, Z. Q. Feng, L. P. Chen, Y. D. Xu, Y. S. Zhao. Dynamic analysis and driving force optimization of a 5-DOF parallel manipulator with redundant actuation. *Robotics and Computer-Integrated Manufacturing*, vol. 48, pp. 51–58, 2017. DOI: [10.1016/j.rcim.2017.02.006](https://doi.org/10.1016/j.rcim.2017.02.006).
- [18] X. F. Liu, J. T. Yao, Y. D. Xu, Y. S. Zhao. Research of

- driving force coordination mechanism in parallel manipulator with actuation redundancy and its performance evaluation. *Nonlinear Dynamics*, vol.90, no.2, pp.983–998, 2017. DOI: [10.1007/s11071-017-3706-8](https://doi.org/10.1007/s11071-017-3706-8).
- [19] Y. M. Song, G. Dong, T. Sun, B. B. Lian. Elasto-dynamic analysis of a novel 2-DoF rotational parallel mechanism with an articulated travelling platform. *Meccanica*, vol. 51, no. 7, pp. 1547–1557, 2015. DOI: [10.1007/s11012-014-0099-3](https://doi.org/10.1007/s11012-014-0099-3).
- [20] B. S. Jiang, H. R. Fang, H. Q. Zhang. Type synthesis and kinematics performance analysis of a class of 3T2R parallel mechanisms with large output rotational angles. *International Journal of Automation and Computing*, vol. 16, no. 6, pp. 775–785, 2019. DOI: [10.1007/s11633-019-1192-9](https://doi.org/10.1007/s11633-019-1192-9).
- [21] J. Guo, G. T. Li, B. Li, S. Wang. A ship active vibration isolation system based on a novel 5-DOF parallel mechanism. In *Proceedings of IEEE International Conference on Information and Automation*, IEEE, Hailar, China, pp.800–805, 2014. DOI: [10.1109/ICInfA.2014.6932761](https://doi.org/10.1109/ICInfA.2014.6932761).
- [22] M. T. Masouleh, C. Gosselin, M. H. Saadatzi, X. W. Kong, H. D. Taghirad. Kinematic analysis of 5-RPUR (3T2R) parallel mechanisms. *Meccanica*, vol. 46, no. 1, pp. 131–146, 2011. DOI: [10.1007/s11012-010-9393-x](https://doi.org/10.1007/s11012-010-9393-x).
- [23] M. T. Masouleh, C. Gosselin, M. Husty, D. R. Walter. Forward kinematic problem of 5-RPUR parallel mechanisms (3T2R) with identical limb structures. *Mechanism and Machine Theory*, vol. 46, no. 7, pp. 945–959, 2011. DOI: [10.1016/j.mechmachtheory.2011.02.005](https://doi.org/10.1016/j.mechmachtheory.2011.02.005).
- [24] M. H. Saadatzi, M. T. Masouleh, H. D. Taghirad. Workspace analysis of 5-PRUR parallel mechanisms (3T2R). *Robotics and Computer-Integrated Manufacturing*, vol. 28, no. 3, pp. 437–448, 2012. DOI: [10.1016/j.rcim.2011.12.002](https://doi.org/10.1016/j.rcim.2011.12.002).
- [25] F. G. Xie, X. J. Liu, J. S. Wang, M. Wabner. Kinematic optimization of a five degrees-of-freedom spatial parallel mechanism with large orientational workspace. *Journal of Mechanisms and Robotics*, vol. 9, no. 5, Article number 051005, 2017. DOI: [10.1115/1.4037254](https://doi.org/10.1115/1.4037254).
- [26] X. L. Wang, B. Zhang, C. J. Li, J. Huang, T. Y. Wu, Y. Cheng. Analysis for global performance index of 5UPS-RPS parallel mechanism based on Jacobian matrix. *Transactions of Beijing Institute of Technology*, vol. 38, no. 9, pp. 899–904, 2018. DOI: [10.15918/j.tbit1001-0645.2018.09.004](https://doi.org/10.15918/j.tbit1001-0645.2018.09.004). (in Chinese)
- [27] X. D. Jin, Y. F. Fang, H. B. Qu, S. Guo. A class of novel 4-DOF and 5-DOF generalized parallel mechanisms with high performance. *Mechanism and Machine Theory*, vol. 120, pp. 57–72, 2018. DOI: [10.1016/j.mechmachtheory.2017.09.015](https://doi.org/10.1016/j.mechmachtheory.2017.09.015).
- [28] X. D. Jin, Y. F. Fang, H. B. Qu, S. Guo. A class of novel 2T2R and 3T2R parallel mechanisms with large decoupled output rotational angles. *Mechanism and Machine Theory*, vol. 114, pp. 156–169, 2017. DOI: [10.1016/j.mechmachtheory.2017.04.003](https://doi.org/10.1016/j.mechmachtheory.2017.04.003).
- [29] C. X. Fan, H. Z. Liu, Y. B. Zhang. Type synthesis of 2T2R, 1T2R and 2R parallel mechanisms. *Mechanism and Machine Theory*, vol. 61, pp. 184–190, 2013. DOI: [10.1016/j.mechmachtheory.2012.10.006](https://doi.org/10.1016/j.mechmachtheory.2012.10.006).
- [30] D. Liang, Y. M. Song, T. Sun, G. Dong. Optimum design of a novel redundantly actuated parallel manipulator with multiple actuation modes for high kinematic and dynamic performance. *Nonlinear Dynamics*, vol. 83, no. 1–2, pp. 631–658, 2016. DOI: [10.1007/s11071-015-2353-1](https://doi.org/10.1007/s11071-015-2353-1).
- [31] J. Wu, Y. Gao, B. B. Zhang, L. P. Wang. Workspace and dynamic performance evaluation of the parallel manipulators in a spray-painting equipment. *Robotics and Computer Integrated Manufacturing*, vol. 44, pp. 199–207, 2017. DOI: [10.1016/j.rcim.2016.09.002](https://doi.org/10.1016/j.rcim.2016.09.002).
- [32] B. B. Zhang, L. P. Wang, J. Wu. Dynamic isotropic performance evaluation of a 3-DOF parallel manipulator. *Journal of Tsinghua University (Science and Technology)*, vol. 57, no. 8, pp. 803–809, 2017. DOI: [10.16511/j.cnki.qhdxxb.2017.22.041](https://doi.org/10.16511/j.cnki.qhdxxb.2017.22.041). (in Chinese)
- [33] H. Q. Zhang, H. R. Fang, B. S. Jiang, S. G. Wang. Dynamic performance evaluation of a redundantly actuated and over-constrained parallel manipulator. *International Journal of Automation and Computing*, vol. 16, no. 3, pp. 274–285, 2019. DOI: [10.1007/s11633-018-1147-6](https://doi.org/10.1007/s11633-018-1147-6).

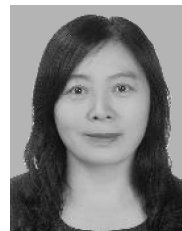


Bing-Shan Jiang received the B.Eng. degree in mechanical electronic engineering from Liaoning Technical University, China in 2015, and the M.Eng. degree in mechanical engineering from Liaoning Technical University, China in 2017. He is currently a Ph.D. degree candidate at School of Mechanical, Electronic and Control Engineering, Beijing Jiaotong University, China.

His research interests include synthesis, kinematics, dynamics and control of parallel robots.

E-mail: 17116381@bjtu.edu.cn

ORCID iD: 0000-0002-9471-8309



Hai-Rong Fang received the B.Eng. degree in mechanical engineering from Nanjing University of Science and Technology, China in 1990, the M.Eng. degree in mechanical engineering from Sichuan University, China in 1996, and the Ph.D. degree in mechanical engineering from Beijing Jiaotong University, China in 2005. She worked as an associate professor

in Department of Engineering Mechanics, Beijing Jiaotong University, China, from 2003 to 2011. She is a professor in School of Mechanical Engineering from 2011 and director of the Robotics Research Center.

Her research interests include parallel mechanisms, digital control, robotics and automation, and machine tool equipment.

E-mail: hrrfang@bjtu.edu.cn (Corresponding author)

ORCID iD: 0000-0001-7938-4737



Hai-Qiang Zhang received the B.Eng. degree in mechanical design and theories from Yantai University, China in 2012, the M.Eng. degree in mechanical engineering from Hebei University of Engineering, China in 2015. He is a Ph.D. degree candidate in mechanical design and theory at Beijing Jiaotong University, China.

His research interests include robotics in computer integrated manufacturing, parallel kinematics machine tool, redundant actuation robots, over-constrained parallel manipulators, and multi-objective optimization design.

E-mail: 16116358@bjtu.edu.cn

ORCID iD: 0000-0003-4421-5671